

Line Resistance Identification-Based Adaptive Droop Control for Distribution Power Loss Minimization of DC Microgrids

Yajie Jiang¹, Yun Yang², Siew-Chong Tan³, and Shu-Yuen Ron Hui⁴

^{1,3,4}Department of Electrical and Electronic Engineering, The University of Hong Kong, Hong Kong, China

²Department of Electrical Engineering, The Hong Kong Polytechnic University, Hong Kong, China

⁴Department of Electrical and Electronic Engineering, Imperial College London, London, U.K.

Email: yjjiang@eee.hku.hk¹, yun1989.yang@polyu.edu.hk², sctan@eee.hku.hk³, ronhui@eee.hku.hk⁴.

Abstract—In this paper, the distribution power loss of DC microgrids comprising both line loss and converter loss is modelled as a quadratic function of current allocation coefficients, which is a convex function with constraints. On basis of convex optimization theory, the optimal current allocation coefficients are on-line calculated by Lagrange multiplier method. Then, an adaptive virtual resistance droop control (AVRDC) is proposed to achieve the given current-sharing rate. In the proposed control, the current-sharing error generates additional adaptive virtual resistance. It is known that the sum of virtual resistance and line resistance should be in inverse proportion to current distribution coefficient. By sampling data of two control periods, the line resistance can be identified in real time. In this way, the real-time efficiency optimization control of DC microgrid can be realized, regardless of line resistance variations. The effectiveness of the proposed control strategy is validated by both simulation and experimental results.

Index Terms—Convex optimization, DC microgrid, distributed energy resource (DER), distribution loss, Lagrange multiplier.

I. INTRODUCTION

In modern smart grid, the reduction of power loss plays an important role in reducing carbon emissions and alleviating the global greenhouse effect. Power savings results in further savings in the facility cooling system because with less heat generated, less heat must be cooled [1]-[6]. The line loss can be theoretically modelled by node voltages and distribution line resistance matrix. For voltage-based model, the optimal voltage references [7] and optimal power flow [8]-[10] of individual DERs can be obtained for achieving on-line power loss reduction. For achieving off-line power loss reduction, optimization methods [7], has been proposed to find the optimal operation point of DERs. However, such offline solutions are effective only in highly ideal operating conditions with little or no parameter variation. In practical scenario where the line resistance is easily affected by the ambient temperature and level of current flow, the performance achieved by the offline solutions are consistently sub-optimal. Besides, only the line loss can be optimized by solutions using the voltage-based loss model. The effect of the power converter loss cannot be described by this model [11].

Apart from the voltage-based loss model, line loss can be directly written as a quadratic function of the line currents. Considering that the line currents are generated by injection currents of DERs, recent works have also considered loss modelling using parameters of the injection currents of DERs. In [12], the converter loss is approximately described as a quadratic function of its output currents. Following this, the converter loss and line loss are modelled as a function of injection currents in the work reported in [13]. However, for this work, the proposed weight droop control method cannot easily consider both the converter loss and the line loss, which results in sub-optimal efficiency. In [14], the author showed that the voltage consensus method can be adopted to reduce the line loss, and subsequently be used to design an optimal controller. However, the converter loss reduction potential is not considered in these works. In practice, the power converter loss may account for over 50% of the overall distribution loss [15]. Therefore, having it taken into consideration in the control scheme would be important in minimizing the distribution power loss.

For dc microgrid with parallel-connected DERs, the output currents of the DERs flow through the respective converters and line resistances, supplying power to the load. The distribution loss of individual DER can be described as a quadratic function of its output currents. The combination of these quadratic functions forms the total distribution loss. Considering the sum of injection currents should be equal to the total load current, the proposed distribution loss model is an equality-constrained convex function with respect to the current allocation coefficients of DERs. In this paper, the Lagrange multiplier method is implemented to find the optimal current allocation combination of the DERs [16], [17]. Then, a centralized adaptive virtual resistance droop control (AVRDC) is proposed to adjust the output currents of DERs according to the optimal current allocation coefficients. In this method, the difference between the currents of each DER and the optimal value are compensated by a proportional-integral (PI) controller to generate a variable virtual resistance, which is added to a static virtual resistance. Then, the adaptive virtual resistance is adopted for the droop controller to provide output voltage references of the local controller. In droop control, the sum of virtual resistance and line resistance is

inversely proportional to current distribution coefficient. By sampling data of two control periods, the line resistance can be identified in real time, which will allow on-line distribution loss minimization of the dc microgrid to be realizable.

II. DISTRIBUTION LOSS MODELLING OF DC MICROGRID

A. Configuration of DC Microgrid

A single-bus dc microgrid is shown in Fig. 1. It comprises distributed generation (DG) units, loads, ESS, and power electronics interfaces. The wind turbine and solar PV panels serve as clean energy. Resistive loads and constant power load (CPL), i.e., motor drive system, are considered in the figure. The ESS is introduced to compensate power and alleviate bus voltage fluctuations. For those DERs, of which injection current can be regulated, such as the ESS, diesel engine, some combinations of ESS and clean energy, are considered as controllable DERs. Other power sources are seen as uncontrollable DERs. For analysis, all uncontrollable DERs and loads are taken as load nodes in the following analysis and are set as constant-current sources in a short time scale.

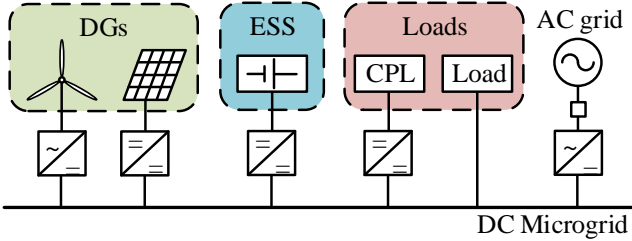


Fig. 1. Configuration of dc microgrid.

B. Distribution Loss Modelling and Convexity Analysis

Taking the simplified dc power system in Fig. 2 as an example, which contains n controllable DERs. Here, R_1, R_2, \dots, R_n , are the distribution line resistances; I_1, I_2, \dots, I_n are the output currents of the DERs; V_1, V_2, \dots, V_n are the output voltages of the DERs; and V_{bus} is the DC bus voltage.

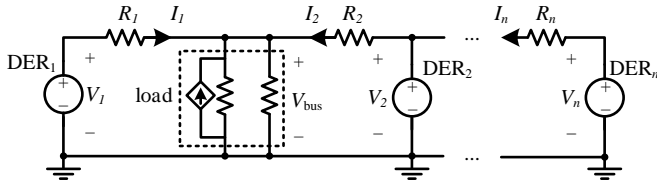


Fig. 2. Simplified circuit of a dc microgrid with n DERs.

For a dc microgrid, the distribution loss contains two parts, namely the converter loss P_{loss}^{conv} and the line loss P_{loss}^{line} . Generally, the converter loss can be simplified as a quadratic expression of the output currents [13], [14]. Then, the distribution power loss of dc microgrid can be written as

$$P_{loss} = P_{loss}^{conv} + P_{loss}^{line} = \sum_{i=1}^n [(a_i + R_i)(I_i)^2 + b_i |I_i| + c_i] \quad (1)$$

where $a_i > 0$, b_i , and c_i are the conversion loss coefficients of i -th converter. The actual dispatchable load current is I_{tol} , which is the difference between total load current and the injection current of uncontrolled DERs. Here, N_1, N_2, \dots, N_n are defined as the current allocation coefficients of the controllable power supplies DER₁, DER₂, ..., DER_n, respectively. In this way, the

distribution loss model can be further written as a function of current allocation coefficients:

$$P_{loss}(N_i) = \sum_{i=1}^n [(R_i + a_i)(N_i I_{tol})^2 + b_i |N_i I_{tol}| + c_i] \quad (2)$$

By considering that the consumed current should be equal to the provided current, yields

$$\sum_{i=1}^n I_i = \sum_{i=1}^n N_i I_{tol} = I_{tol} \Rightarrow g(N_i) = \sum_{i=1}^n N_i = 1 \quad (3)$$

By taking the second partial derivative of equation (2) with respect to the N_i

$$\frac{\partial P_{loss}(N_i)}{\partial N_i} = 2N_i(I_{tol})^2(R_i + a_i) + b_i |I_{tol}| \geq 0 \quad (4.1)$$

$$\frac{\partial^2 P_{loss}(N_i)}{\partial N_i^2} = 2(I_{tol})^2(R_i + a_i) \geq 0 \quad (4.2)$$

Thus, the distribution power loss model in (2) is strictly convex. Then, the objective function and constraints of the proposed control strategy can be given as

$$\begin{aligned} & \text{minimize} && J = P_{loss}(N_i) \\ & \text{subject to} && \sum_{i=1}^n N_i = 1, P_{\min i} \leq P_i \leq P_{\max i} \end{aligned} \quad (5)$$

where $P_{\min i}$ and $P_{\max i}$ are lower and upper bounds of the power generation capacities.

III. PROPOSED CONTROL STRATEGY

A. Lagrange Multiplier Method for Convex Optimization

A geometric illustration of the equality constrained optimization problem (5) is presented in Fig. 3, where the feasible set $g(N_i)$ and the level sets of the convex function $P_{loss}(N_i)$ can be seen graphically. Here, the Lagrange multiplier is selected to find the optimal current allocation coefficients.

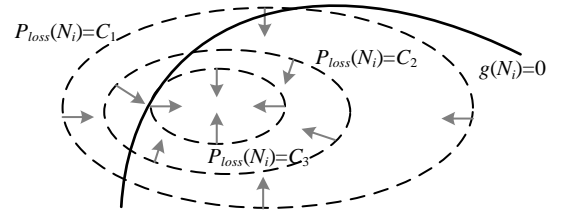


Fig. 3. Sketch map of the proposed convex optimization with constraint.

Based on (5), a Lagrange multiplier variable $\lambda \neq 0$ is introduced and the Lagrange function is defined as

$$\begin{aligned} L(N_i, \lambda) &= P_{loss}(N_i) + \lambda \cdot g(N_i) \\ &= \sum_{i=1}^n [(a_i + R_i)(N_i I_{tol})^2 + b_i |N_i I_{tol}| + c_i] + \lambda (\sum_{i=1}^n N_i - 1) \end{aligned} \quad (6)$$

The optimal current allocation coefficients (i.e., N_i) can be derived by equalizing the first-order partial derivative of the Lagrange function to zero, as

$$\nabla_{N_i, \lambda} L(N_i, \lambda) = \left(\frac{\partial L}{\partial N_i}, \frac{\partial L}{\partial \lambda} \right) = 0 \quad (7)$$

which yields

$$N_i = -\frac{b_i |I_{tol}| + \lambda}{2(a_i + R_i)(I_{tol})^2} \quad (8.1)$$

$$\lambda = -\sum_{i=1}^n \frac{b_i}{2(a_i + R_i)|I_{tol}|} + 1 \Big/ \sum_{i=1}^n \frac{1}{2(a_i + R_i)(I_{tol})^2} \quad (8.2)$$

Considering the output power constraint in (5), the optimal current allocation coefficients derived can be given as

$$N_i = \begin{cases} I_{\max i} / I_{\text{tol}} & P_i > P_{\max i} \\ I_{\min i} / I_{\text{tol}} & P_i < P_{\min i} \\ N_i(k+1) & P_{\min i} \leq P_i \leq P_{\max i} \end{cases} \quad (9)$$

where $I_{\min i}$ and $I_{\max i}$ are the lower and upper bound output currents of the i -th DER, which can be calculated by the voltage and power bound. If the output power of the i -th DER reaches the limits (i.e., $P_{\max i}$ or $P_{\min i}$), it can operate at the limited power while the power loss of rest DER systems is still a convex function such that the optimization control strategy can still be used to minimize the distribution power loss.

B. Adaptive Virtual Resistance Droop Control and Line Resistance Identification

With regards to line resistance variation, to achieve loss minimization, two operations must be performed: the allocation of the output currents according to (8) and the real-time distribution line resistance identification. The control block diagram is shown in Fig. 4.

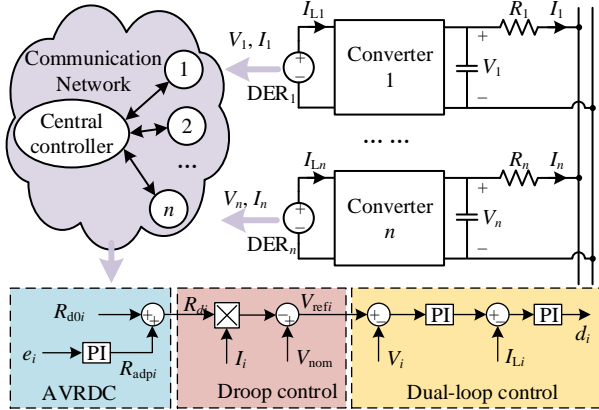


Fig. 4. Control block diagram of the AVRDC.

Here, the virtual resistance of the droop control comprises a static virtual resistance R_{d0i} and an adaptive virtual resistance R_{adpi} , and is given by

$$R_{di} = R_{d0i} + R_{adpi} \quad (10)$$

By defining $x_i = I_i/N_i$, current allocation error is written as $e_i = \sum_{i \neq j}^n (x_i - x_j)$. Then, the adaptive virtual resistance can be derived by a PI controller using

$$R_{adpi} = (k_{pi} + k_{ii} / s)e_i \quad (11)$$

where k_{pi} and k_{ii} are the proportional and integral gains of i th PI controller. Finally, the reference voltage by using droop control is given as

$$V_{refi} = V_{\text{nom}} - R_{di} I_i \quad (12)$$

where V_{nom} is the nominal bus voltage. As shown in Fig. 4, the operating principle of the proposed AVRDC is illustrated as follows. When x_i is greater than those of other nodes x_j , the virtual resistance of the i th converter R_{adpi} will be increased (I_i is decreased) and R_{adpj} will be decreased (I_j is increased) to make $I_i/N_i = I_j/N_j$. On the contrary, if x_i is less than x_j , the virtual resistance of the i th converter, R_{adpi} will be decreased and R_{adpj} will be increased. The R_{di} results in the adaptive

reference V_{refi} , is adopted as the output voltage reference for the dual-loop control. Consequently, the output currents of DERs are distributed based on the given allocation coefficients at steady state. The current allocation of DERs can be achieved with variable equivalent resistances. According to the principle of droop control, we have

$$\begin{aligned} V_{\text{nom}} - (R_i + R_{di})I_i &= V_{\text{bus}} = V_{\text{nom}} - (R_j + R_{dj})I_j \\ \Rightarrow \frac{I_i}{I_j} &= \frac{N_i}{N_j} = \frac{R_j + R_{dj}}{R_i + R_{di}} \end{aligned} \quad (13)$$

As shown in (13), the allocation coefficient of each converter is inversely proportional to its sum of line resistance and virtual resistance. In this way, we can get $n-1$ equations by sampling once, i.e., kT . T is the algorithm execution period, which should be set long enough to ensure that the adaptive virtual resistance reaches a stable value. Among the equations, the current allocation coefficient N_i and virtual resistance $R_{di} = R_{d0i} + R_{adpi}$ is known, while the distribution line resistance R_i is unknown. To get the unknown variable R_i , we should sample twice, i.e., k and $k-1$:

$$\begin{cases} \frac{R_i + R_{di}^k}{R_j + R_{dj}^k} = \frac{R_i + R_{d0i} + R_{adpi}^k}{R_j + R_{d0j} + R_{adpj}^k} = \frac{N_j^k}{N_i^k} \\ \frac{R_i + R_{di}^{k-1}}{R_j + R_{dj}^{k-1}} = \frac{R_i + R_{d0i} + R_{adpi}^{k-1}}{R_j + R_{d0j} + R_{adpj}^{k-1}} = \frac{N_j^{k-1}}{N_i^{k-1}} \end{cases} \quad (14)$$

With the $2(n-1)$ equations, the n distribution line resistances of DERs can be obtained. The time sequence of identification is given in Fig. 5. As shown in the figure, the adaptive virtual resistance R_{adpi}^k corresponding to k time current allocation coefficient N_i^k , can only be obtained at the $k+1$ time.

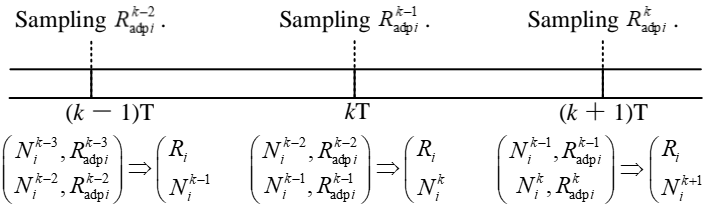


Fig. 5. Time sequence of the line resistance identification.

IV. CASE STUDIES

Two simulation case studies and one experimental case are conducted to verify the effectiveness of the proposed method. The main parameters of the microgrid are listed in Table I. The algorithm execution period is set as 10 s. The proportional and integral gains of the PI controllers in the dual-loop control are kept constant for all the cases of the simulation. For power supply nodes 1, 2, 3, 4, the coefficients of their converter loss [a , b , c as (1)] are given in Table II.

TABLE I. MAIN PARAMETERS OF DC MICROGRID

Parameters	Value
Battery pack voltage (V_{bus})	48 V
Total load current (I_{tol})	15 A
Line resistance of DER ₁ (R_1)	0.5 Ω
Line resistance of DER ₂ (R_2)	0.8 Ω
Line resistance of DER ₃ (R_3)	0.2 Ω
Line resistance of DER ₄ (R_4)	1.1 Ω

TABLE II. CONVERTER LOSS COEFFICIENTS

Converter number	a	b	c
1	1.166	2.410	1.110
2	0.176	1.040	2.040
3	0.477	0.956	1.360
4	0.730	1.600	0.600

A. Convexity Verification of Distribution Loss Model

To further illustrate the characteristics of the proposed current-based distribution loss model, the loss waveforms of a dc microgrid under different load currents are plotted in Fig. 6 and Fig. 7. Using the parameters of DER₁ and DER₂ in Table I and II, Fig. 6 shows the curves of power loss with two DERs under variation of current distribution coefficients. Under the constraint, there is one controllable variable (N_1 or N_2), which results in a two-dimensional curve. In Fig. 6, the curve is up-opening conic regardless the variation of load current. Using the parameters of DER₁, DER₂ and DER₃ (Fig. 7(a) and (b)) and DER₂, DER₃ and DER₄ (Fig. 7(c) and (d)), Fig. 7 shows the waveforms of power loss with three DERs. With two controllable variables, the distribution loss is a three-dimensional waveform. In the figures, the proposed loss model maintains the convexity (smooth and has only one minimum point) regardless of the load power level or the range of current allocation coefficients. For more DERs, the convexity is proven by (4).

B. Case 1: Method Implementation

Fig. 8 shows the waveforms of the voltages, output currents, current allocation coefficients, identified line resistances, adaptive virtual resistances, and distribution power loss for Case 1.

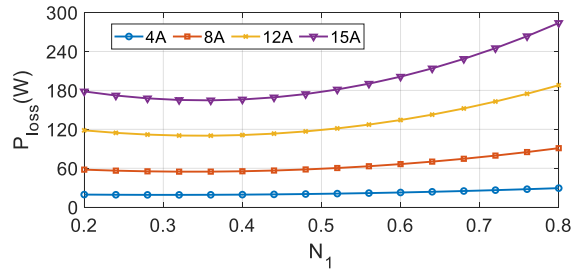


Fig. 6. Distribution loss with two DERs under variation of current allocation coefficients, 4A, 8A, 12A, and 15A.

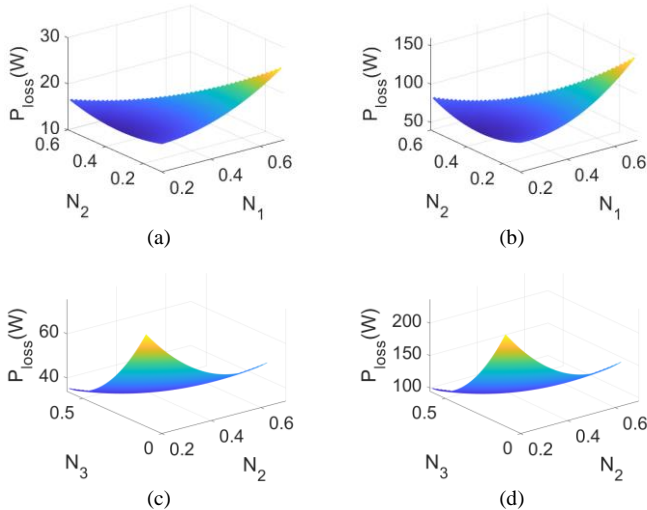


Fig. 7. Distribution loss with three DERs under variation of current allocation coefficients for load currents (a) 4 A, (b) 12 A, (c) 8 A, and (d) 15 A.

adaptive virtual resistances, virtual resistances, and the distribution power loss for Case 1. Here, the conventional droop control with static virtual resistances, ($R_{d01} = R_{d02} = R_{d03} = R_{d04} = 0.2\Omega$) are adopted for the four DERs in the period of 0 to 2 s. Without optimization, the distribution loss is 96.76 W. To obtain the data of two periods, average current allocation ($N_1: N_2: N_3: N_4 = 1: 1: 1: 1$) is adopted by the proposed AVRDC in the period of 2 s to 12 s. It is shown that the current allocation can be achieved with the AVRDC. Under average current allocation, the total distribution loss is increased to 100.04W: the converter loss is reduced, while the line loss is increased. After getting enough data, the line resistances are calculated at time = 12 s. Then, the optimal current allocation coefficients are obtained. Concurrently, they are used to allocate currents by AVRDC. Finally, the distribution loss is reduced to 86.40W. Some control results of Case 1 are given in Table III. It is shown that the line resistances can be accurately identified. Moreover, the actual

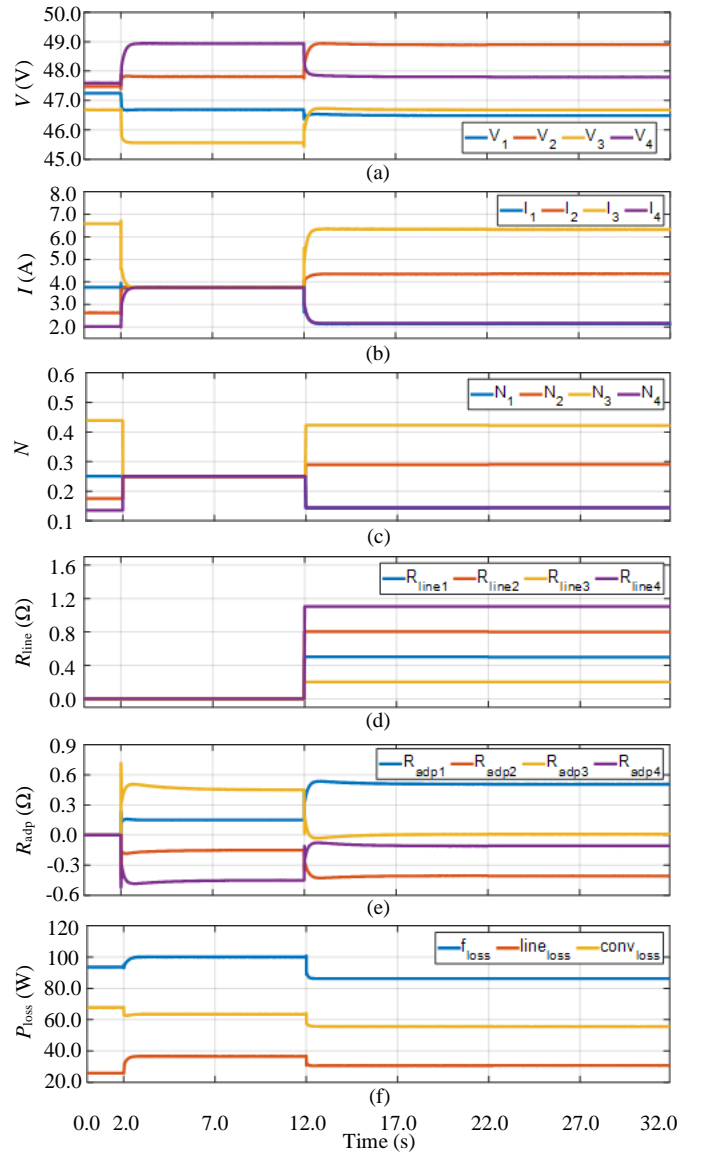


Fig. 8. Waveforms of the (a) voltages, (b) output currents, (c) current allocation coefficients, (d) identified line resistances, (e) adaptive virtual resistances, and (f) distribution power loss for Case 1.

optimal current allocation coefficients are consistent with the theoretical optimal values.

TABLE III. CONTROL RESULTS OF CASE 1

Line resistance	Actual value	Identified value	Current allocation coefficients	Theoretical optimal value	Actual optimal value
R_1	0.5 Ω	0.5000 Ω	N_1	0.1426	0.1430
R_2	0.8 Ω	0.8004 Ω	N_2	0.2902	0.2908
R_3	0.2 Ω	0.2028 Ω	N_3	0.4226	0.4217
R_4	1.1 Ω	1.1051 Ω	N_4	0.1446	0.1445

C. Case 2: Line Resistance Variation

In this case, the dynamic performance of the proposed method under line resistance variation is studied, and the results are given in Fig. 9. The proposed control strategy is adopted for the microgrid during the entire period of 0 to 42 s. The static virtual resistances are $R_{d01} = -0.1 \Omega$, $R_{d02} = 0.3 \Omega$, $R_{d03} = 0.1 \Omega$, and $R_{d04} = 0.3 \Omega$. The distribution line resistances, R_1 and R_3 are changed from the nominal values in

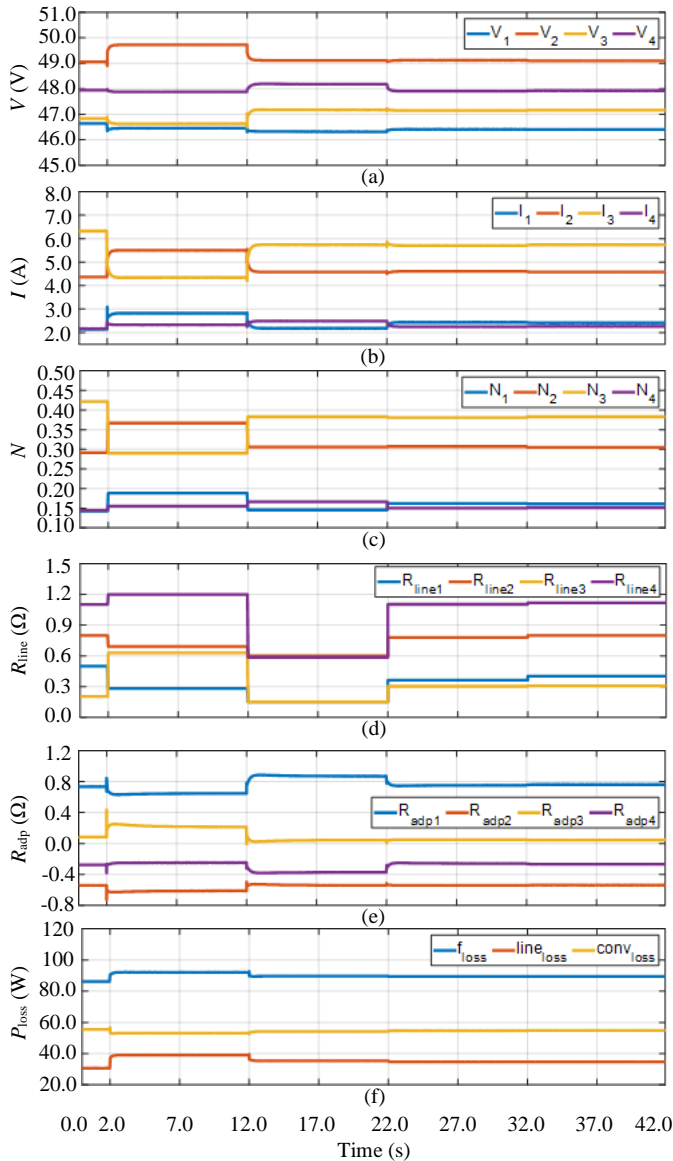


Fig. 9. Waveforms of the (a) voltages, (b) output currents, (c) current allocation coefficients, (d) identified line resistances, (e) adaptive virtual resistances, and (f) distribution power loss for Case 2.

Table I to 0.4 Ω , and 0.3 Ω , respectively at 2 s. Then, the distribution line resistance identification error is generated using the former data. Meanwhile, the current allocation coefficients also fluctuate from their optimal values. After two periodic iterations, line resistance is precisely obtained using the updated data at time = 22 s. Then, the distribution loss minimization for the dc microgrid at 89.61 W is achieved again during the period of 22 s to 42 s. Some control results of Case 2 are given in Table IV. Clearly, the line resistances can be accurately identified even though it is a varying line resistance. Due to the change in line resistances, the optimal current allocation coefficients in Table IV are different from that of Table III. Also, the actual optimal current allocation coefficients are consistent with the theoretical optimal values.

TABLE IV. CONTROL RESULTS OF CASE 2

Line resistance	Actual value	Identified value	Current allocation coefficients	Theoretical optimal value	Actual optimal value
R_1	0.4 Ω	0.4012 Ω	N_1	0.1600	0.1605
R_2	0.8 Ω	0.7993 Ω	N_2	0.3035	0.3047
R_3	0.3 Ω	0.3060 Ω	N_3	0.3848	0.3831
R_4	1.1 Ω	1.1040 Ω	N_4	0.1517	0.1518

D. Case 3: Experimental Verification

Experiments are conducted on a 48 V DC microgrid with three DER systems being connected to the DC bus. The main parameters are provided in [2]. Digital signal processor (DSP) Delfino TMS320F28379D is adopted as the controllers for the DER systems. The converter loss curves of the three grid-connected boost converters are plotted in Fig. 10. The conversion loss coefficients for the DER1, DER2 and DER3 are $a_1 = 1.161$, $b_1 = 0.730$, $c_1 = 1.693$, $a_2 = 0.641$, $b_2 = 0.547$, $c_2 = 5.260$, and $a_3 = 1.693$, $b_3 = 5.26$, and $c_3 = 3.54$.

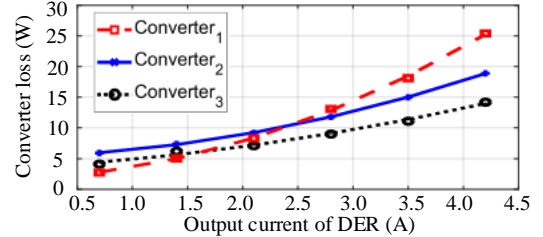


Fig. 10. Converter loss versus output currents of DER systems in experiment.

The conventional control strategy, average current distribution and the proposed control strategy are adopted during the period from 0s to 6s, from 6s to 12s, and from 12s to 20s, respectively. The total output current is $I_{o1}=4.75$ A. Fig. 11 show the waveforms of current allocation coefficients, identified line resistances, output currents of the DERs, and distribution power loss of the DC microgrid. The internal variables, i.e., current allocation coefficients, line resistances, power loss are output via the digital-to-analog (DAC) pins of the DSP. When the proposed control strategy is adopted at the 12s, the Lagrange multiplier is calculated to be -40.61 and the corresponding current allocation coefficients are 0.342, 0.517 and 0.141, respectively, as shown in Fig. 11(a). As shown in Fig. 11(b), the line resistances $R_1 = 1.21\Omega$, $R_2 = 0.96 \Omega$, and $R_3 = 1.04 \Omega$ are obtained at 12s. The measured output currents of the DER systems are 1.62 A, 2.46 A and 0.67 A, as shown

in Fig. 11(c). Obviously, the output currents of the DER systems are well-regulated by the adaptive droop control to track the references. The distribution power loss are 34.43 W, 34.72 W and 30.67 W, respectively. Control results of case 3 are given in Table V.

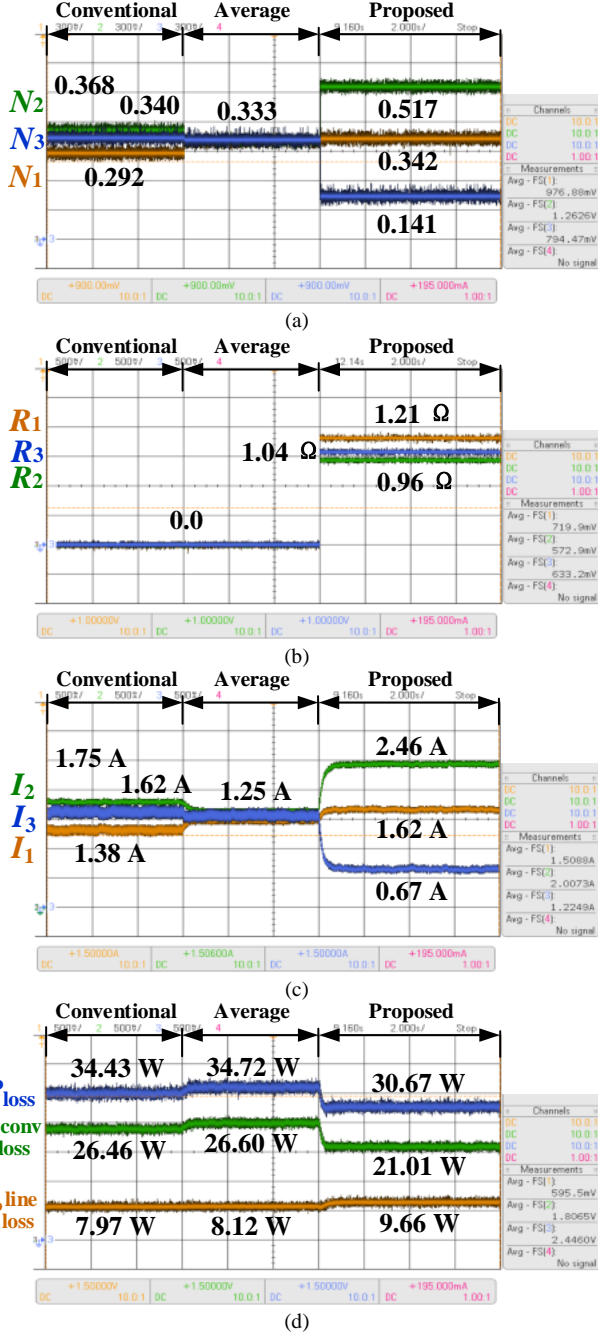


Fig. 11. Waveforms of the (a) current allocation coefficients, (b) identified line resistances, (c) output currents, and (d) distribution power loss of the DC microgrid for Case 3.

TABLE V. CONTROL RESULTS OF CASE 3

Line resistance	Actual value	Identified value	Current allocation coefficients	Theoretical optimal value	Actual optimal value
R_1	1.208 Ω	1.21 Ω	N_1	0.349	0.342
R_2	0.974 Ω	0.96 Ω	N_2	0.524	0.517
R_3	1.07 Ω	1.04 Ω	N_3	0.127	0.141

Fig. 12 presents a comparison of the distribution power loss of the system with the conventional optimization control, with droop control (average current distribution) and that with the proposed control. Compared with the method that considers only the line loss, the total distribution power loss are reduced by 10.71% in Case 1, 13.17% in Case 2, and 10.92% in Case 3, with the proposed control. With the proposed control, the distribution power losses are reduced by 13.94% in Case 1, 29.66% in Case 2, and 11.66% in Case 3, as compared to that with conventional droop control.

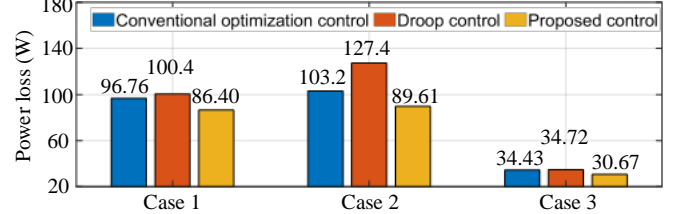


Fig. 12. Comparison of the distribution loss of the system with conventional optimization control, with droop control, and that with the proposed control.

V. CONCLUSIONS

In this paper, the distribution power loss of radial dc network is modelled as a quadratic function of the current distribution coefficients. It is proved that the loss is an equality-constrained convex function with respect to the current distribution coefficients. The Lagrange multiplier method is used to find the optimal current distribution coefficient in real time. An AVRDC to achieve distribution loss minimization for DC microgrid is presented. Meanwhile, the line resistance can be identified by solving the equation of virtual resistance and current allocation coefficients. Consequently, optimal current sharing for distribution loss minimization can be achieved regardless of the distribution line resistances or load variation. The effectiveness has been verified via simulation and experimental results.

REFERENCES

- [1] Y. Yang, S. C. Tan, and S. Y. R. Hui, "Mitigating distribution power loss of DC microgrids with DC electric springs," *IEEE Trans. Smart Grid*, vol. 9, no. 6, pp. 5897-5906, Nov. 2018.
- [2] Y. Jiang, Y. Yang, S. C. Tan, and S. Y. R. Hui, "Adaptive current sharing of distributed battery systems in DC microgrids using adaptive virtual resistance-based droop control," in *Proc. 2019 IEEE Energy Conversion Congress & Expo. (ECCE)*, Baltimore, USA, Sept. 2019, pp. 4262-4267.
- [3] J. Deng, Y. Mao, and Y. Yang, "Distribution power loss reduction of standalone DC microgrids using adaptive differential evolution-based control for distributed battery systems," *Energies*, vol. 13, no. 9, Apr. 2020.
- [4] Y. Yang, Y. Qin, S. C. Tan, and S. Y. R. Hui, "Efficient improvement of photovoltaic-battery systems in standalone DC microgrids using a local hierarchical control for the battery system," *IEEE Trans. Power Electron.*, vol. 34, no. 11, pp. 10796-10807, Nov. 2019.
- [5] Y. Yang, Y. Qin, S. C. Tan, and S. Y. R. Hui, "Reducing distribution power loss of islanded AC microgrids using distributed electric springs with predictive control," *IEEE Trans. Ind. Electron.*, vol. 67, no. 10, pp. 9001-9011, Nov. Feb. 2020.
- [6] Y. Jiang, Y. Yang, S. C. Tan, and S. Y. Ron Hui, "Distribution power loss mitigation of parallel-connected distributed energy resources in low-voltage DC microgrids using a Lagrange multiplier-based adaptive droop control," *IEEE Trans. Power Electron.*, Jan. 2021, early access.

- [7] Q. Nguyen, H. V. Padullaparti, K. W. Lao, S. Santoso, X. Ke, and N. Samaan, "Exact optimal power dispatch in unbalanced distribution systems with high PV penetration," *IEEE Trans. Power Syst.*, vol. 34, no. 1, pp. 718-728, Sept. 2018.
- [8] X. Qian, Y. Yang, C. Li, and S. C. Tan, "Operating cost reduction of DC microgrids under real-time pricing using adaptive differential evolution algorithm," *IEEE Access*, vol. 8, pp.169247-169258, Sept. 2020.
- [9] X. Qian, Y. Yang, C. Li, and S. C. Tan, "Economic dispatch of DC microgrids using real-time pricing using adaptive differential evolution algorithm," in *IEEE 9th International Power Electronics and Motion Control Conference*, Nanjing, China, Nov. 2020, pp. 1114-1120.
- [10] A. Garcés, "On the convergence of Newton's method in power flow studies for DC microgrids," *IEEE Trans. Power Syst.*, vol. 33, no. 5, pp. 5770-5777, Sept. 2018.
- [11] C. Gavriluta, I. Candela, A. Luna, A. Gomez-Exposito, and P. Rodriguez, "Hierarchical control of HV-MTDC systems with droop-based primary and OPF-based secondary," *IEEE Trans. Smart Grid*, vol. 6, no. 3, pp. 1502-1510, May 2015.
- [12] J. Beerten, S. Cole, and R. Belmans, "Generalized steady-state VSC MTDC model for sequential AC/DC power flow algorithms," *IEEE Trans. Power Syst.*, vol. 27, no. 2, pp. 821-829, May 2012.
- [13] H. Su, C. Deng, F. Guo, X. Chen, and C. Qi, "Distributed load sharing and transmission power loss optimisation for DC microgrids," *IET Control Theory*, vol. 13, no. 17, pp. 2930-2939, Appl. 2019.
- [14] J. Ma, L. Yuan, Z. Zhao, and F. He, "Transmission loss optimization-based optimal power flow strategy by hierarchical control for DC microgrids," *IEEE Trans. Power Electron.*, vol. 32, no. 3, pp. 1952-1963, Mar. 2017.
- [15] H. Kakigano, Y. Miura, T. Ise, J. Van Roy, and J. Driesen, "Basic sensitivity analysis of conversion losses in a DC microgrid," In *2012 International Conference on Renewable Energy Research and Applications (ICRERA)*. IEEE, Nov. 2012, pp. 1-6.
- [16] Y. Jiang, Y. Yang, S.C. Tan, and S.Y. Ron Hui, "Distributed sliding mode observer-based secondary control for DC microgrids under cyber-attacks," *IEEE, J. Emer. Sel. Top. Circuits Syst.*, vol. 11, no. 1, pp. 144-154, Mar. 2021.
- [17] S. Boyd and L. Vandenberghe, *Convex Optimization*. Cambridge, U.K.: Cambridge Univ. Press, 2004.